AIAA JOURNAL
Vol. 44, No. 12, December 2006

Sensitivity Analysis and Optimal Design of Smart Piezolaminated Composite Beams

R. Sedaghati,* A. Zabihollah,‡ and M. Ahari‡
Concordia University, 1515 St. Catherine West, Montreal, Quebec H3G 2W1, Canada

DOI: 10.2514/1.21564

The static and dynamic interaction between piezoelectric layer and host laminated beam has been investigated using classical laminate theory and first-order shear deformation theory. A finite element model has been developed to study the mechanical and electrical behavior of laminated composite beam with piezoelectric actuators. The numerical results have been compared with those available in the literature in order to validate the accuracy of the model. A design optimization methodology has been developed by combining the finite element model and the sequential quadratic programming technique to improve the structural performance. Further, the optimization algorithm has been improved by performing the sensitivity analysis and analytical gradients of constraints and objective function. Various types of optimization problems including shape control of a beam and mass minimization have been investigated. By careful positioning of the actuators and polarizing them to create bending moment and stretching force when required, a very precise shape control has been achieved as well as considerable reduction in the mass of the structure. It has been observed using the analytical gradients of constraints and objective function analytically can significantly reduce the total number of iteration required to obtain the optimal design.

Nomenclature

b	=	width of the beam
C_{ij}	=	material coefficients
D_{11}	=	coefficients of bending stiffness matrices
d_{ij}	=	piezoelectric constant
$\{E\}$	=	electric field vector
E_i	=	Young's moduli in i direction
$\{F\}^e$	=	element force vector
F^P	=	bending force due to the piezoelectric actuator
G_{ij}	=	shear moduli in the ij plane
$[G]^e$	=	element's geometric stiffness matrix
h	=	height of the beam
I_1, I_2	=	mass moment of inertias
$[K]^e$	=	element's stiffness matrix
l	=	length of the beam
M_x	=	bending moment about the y axis
M_x^P	=	piezoelectric moment
$[M]^e$	=	element's mass matrix
N	=	total number of plies in the laminate
n_p	=	number of piezoelectric layers in the laminate
P_x^P	=	axial piezoelectric force
$\bar{Q}_{ij}$	=	plane stress-reduced stiffness
Q_x^P	=	transverse shear force due to piezoelectric actuator
S_i	=	displacement shape functions
t_k	=	thickness of individual ply in the laminate
u	=	displacement in x direction
$V^{(k)}$	=	applied voltage
w	=	deformation in the thickness direction
θ	=	angle between fiber orientation and the reference axis
μ	=	shear correction factor
ν_{ij}	=	Poisson's ratio
ρ	=	density
$\sigma_{ij}, \varepsilon_{ij}$	=	stress and strain components
φ_i	=	rotation shape functions f
ω	=	natural frequency

Received 5 December 2005; revision received 27 April 2006; accepted for publication 17 July 2006.

*Assistant Professor, Department of Mechanical and Industrial Engineering; sedagha@alcor.concordia.ca (corresponding author).
‡Graduate Student, Department of Mechanical and Industrial Engineering.
‡Graduate Student, Department of Mechanical and Industrial Engineering.

I. Introduction

THE concept of using sensors and actuators to design a self-controlling and self-monitoring smart laminated composite structure has drawn considerable interest among the research community. The advantage of incorporating these types of materials into the structures can combine the superior mechanical properties of laminated composites and sensing and actuating capabilities of piezoelectric materials [1]. The development of smart laminated composite structures with adaptive capabilities may further improve the performance and reliability of the laminated structure. Design optimization of smart structures is a recent research thrust. Although many analysis models have been developed, they are often combined with heuristic design methods or informal optimization procedures.

Soares et al. [2] applied sensitivity analysis and optimization techniques to maximize the effect of piezoelectric actuator and minimize the weight of the structure. Correia et al. [3] presented a model to optimize the lamination schemes of the adaptive composite structures with surface bonded piezoelectric actuators. The design variables in this study were considered as layer thickness, actuator size and location of piezoelectric layers. Birman [4] presented the optimal design of a sandwich plate with embedded piezoelectric materials to minimize the transverse static deflection. Bruant et al. [5] developed a model to determine the optimal location of piezoelectric actuator by minimizing the mechanical energy of the system and sensor location by maximizing the energy of the state output. Soares et al. [6] presented a finite element model based on the higher-order shear displacement field to the optimal design of laminated composite plate structures. The objective of optimization in this work was the determination of the optimum location of the piezoelectric actuators in order to maximize their efficiency for static deformation. Yan and Yam [7] considered the bending moment induced by piezoelectric patch actuators as objective function to investigate the optimal thickness and embedded depth of piezoelectric actuators in order to maximize the piezoelectric actuating force in active vibration control applications. Barboni et al. [8] modeled the bending moment produced by single actuator using the pin-force model and optimized size and position of the actuators using an analytical method. Batra and Geng [9] studied the transient elastic deformations of a plate with piezoceramic element bonded to the top and bottom surfaces and analyzed the effect of the shape and size of the

piezoceramic actuators on increasing the buckling load of the plate. Correia et al. [10] found the optimal location of the integrated piezoelectric actuators and also fiber angles to maximize the buckling load of the adaptive plate structures. Baz and Poh [11] solved the problem of optimal placement of a preselected actuator size. They used beam element to model a cantilever beam and included the mass and the stiffness of the actuator in the beam model. Aldraihem [12] optimized the size and location of single or two pairs of actuators based on the beam modal cost and controllability index. Suleman and Goncalves [13] used physical programming to perform multiobjective optimization of an adaptive composite beam with piezoelectric actuators bonded on the top and bottom surfaces of the beams to optimize the size and placement of the actuators pairs. The objective function was maximization of the performance of the actuators, minimization of the mass of the actuators and minimization of the actuation voltage. For other advances in optimization of smart structures one may consult the survey done by Frecker [14] who reviewed the most recent publications in this subject.

The present work intends to develop analytical sensitivity analysis and formal design optimization methodology to improve the performance of adaptive laminated composite beams with piezoelectric actuator patches, as shown in Fig. 1. Various optimization problems have been investigated under stress, displacement and frequency constraints. Analytical formulations based on the finite element method using classical laminate and first-order shear deformation theories have been developed to find gradient of the constraints. These gradients are then used to establish the formal design optimization algorithm. In the following, the finite element analysis of the smart laminated composite beam based on the classical lamination theory and the first-order shear deformation theory will be briefly explained. Next, the formal design optimization formulation based on sequential quadratic programming (SQP) technique is described. This follows by gradient evaluations of constraints for static and frequency problems. Finally, some illustrative examples are presented.

II. Finite Element Analysis of Laminated Smart Beams

The governing equation of a lamina including piezoelectric effect is given by

$$\{\sigma\} = [C]\{\varepsilon\} - [e]^T\{E\} \tag{1}$$

where $\{\sigma\}$, $\{\varepsilon\}$, $\{E\}$, $[C]$, and $[e]$ represent the stress vector, the strain vector, the electric field vector, the elasticity constant, and the piezoelectric constant matrices, respectively. Stresses in the kth layer of the smart laminated beams can be computed by considering only the axial and through the thickness components in the 3-D stress-strain equation and by considering constant displacements through the thickness as follows:

$$\begin{Bmatrix} \sigma_x \\ \tau_{xz} \end{Bmatrix}_k = \begin{bmatrix} \bar{Q}_{11} & 0 \\ 0 & \bar{Q}_{55} \end{bmatrix}_k \begin{Bmatrix} \varepsilon_x \\ \gamma_{xz} \end{Bmatrix}_k - \begin{Bmatrix} e_{31} \\ 0 \end{Bmatrix}_k E_z^k \tag{2}$$

where $\bar{Q}_{ij}$ is the reduced coefficient of stiffness matrix, e_{31} is the piezoelectric constant which can be determined as $e_{31} = \bar{Q}_{11}d_{31}$, b is the width of the beam; and E_z is the electric filed vector in thickness direction which is defined as $E_z = V/t_p$ where, V is the applied voltage and t_p is the thickness of piezoelectric layer. It should be noted that the piezoelectric is considered as an isotropic materials. Therefore, the angle orientation does not change its materials properties. In the following sections the finite element formulation for static and dynamic analysis of smart laminated beams based on two single-layer theories, namely, classical laminate theory and first-order shear deformation theory have been presented.

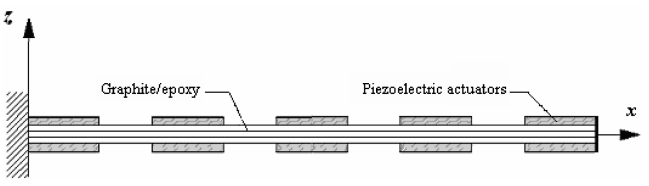

Fig. 1 Schematic illustration of piezolaminated composite beam.

A. Classical Laminate Theory

According to the classical laminate theory, displacement field is given by

$$u(x,z,t) = u_0(x,t) + z\frac{\partial w_0}{\partial x}, \qquad w(x,z,t) = w_0(x,t) \tag{3}$$

where t is the time and (u_0, w_0) are the displacements along the coordinate lines of a material point on the midplane (xy plane). By neglecting the shear effects, the strain field can be determined as

$$\varepsilon_x = \varepsilon_x^0 + z\kappa_x, \qquad \gamma_{xz} = 0, \quad \text{where } \varepsilon_x^0 = \frac{\partial u_0}{\partial x}, \qquad \kappa_x = \frac{\partial^2 w_0}{\partial x^2} \tag{4}$$

Substituting Eq. (4) into Eq. (2), and integrating through the thickness, the stress resultants can be obtained as [15]:

$$\begin{Bmatrix} P_x \\ M_x \end{Bmatrix} = \begin{bmatrix} \bar{A}_{11} & \bar{B}_{11} \\ \bar{B}_{11} & \bar{D}_{11} \end{bmatrix} \begin{Bmatrix} \varepsilon_x^0 \\ \kappa_x \end{Bmatrix} - \begin{Bmatrix} P_x^p \\ M_x^p \end{Bmatrix} \tag{5}$$

where

$$\{\bar{A}_{11} \quad \bar{B}_{11} \quad \bar{D}_{11}\} = \sum_{k=1}^{n} \int_{z_{k-1}}^{z_k} \bar{Q}_{11}(1, z, z^2)\, \mathrm{d}z \tag{6}$$

where z_k is measured from the midplane of the laminate and $z_0 = -h/2$ and $z_n = h/2$ where h is the total thickness of the laminate. It should be noted that for symmetric laminate $\bar{B}_{11} = 0$ and $\bar{D}_{11}$ can be expressed as [16]:

$$\bar{D}_{11} = \sum_{k=1}^{n} \bar{Q}_{11}\left(t_k\bar{z}_k^2 + \frac{t_k^3}{12}\right) \tag{7}$$

where $\bar{z}_k$, the distance from the midplane surface to the middle of kth ply. The force and moment resultants due to piezoelectric actuators are given by Eqs. (8a) and (8b), respectively [15]:

$$P_x^p = \sum_{k=1}^{n+n_p} \int_{z_{k-1}}^{z_k} b\bar{Q}_{11}^{(k)} d_{31}^{(k)} E_z^{(k)}\, \mathrm{d}z \tag{8a}$$

$$M_x^p = \sum_{k=1}^{n+n_p} \int_{z_{k-1}}^{z_k} b\bar{Q}_{11}^{(k)} d_{31}^{(k)} E_z^{(k)} z\, \mathrm{d}z \tag{8b}$$

where n_p is the number of surface bounded piezoelectric actuators. It is noted that piezoelectric actuators are bounded to the top and bottom surfaces of the beam and for non piezoelectric layers P_x^p and M_x^p are zero. The equation of motion can be derived using the Hamilton principle as

$$\int_0^T (\delta U + \delta V - \delta K)\, \mathrm{d}t = 0 \tag{9}$$

where $U = U_s + U_p$ is the virtual strain energy, V is the work done by the applied force and K is the kinetic energy, U_s is the strain energy, and U_p is the electrical field energy of piezoelectric layers. Using the finite element method and Hamilton principle in Eq. (9), the discrete matrix equation of motion in the smart laminated beam is derived as [15]:

$$[M]^e\{\ddot{w}\}^e + ([K]^e + [G]^e)\{w\}^e = \{F\}^e + \{F^P\}^e \tag{10}$$

where $[K]^e$, $[G]^e$, and $[M]^e$ represent element stiffness, geometric stiffness and mass matrices, respectively. $\{w\}^e$ and $\{F\}^e$ are the element nodal displacements and the external force vector,

respectively. The force components due to the piezoelectric actuators, $\{F^P\}^e$ can be obtained as

$$F_i^P = \int_0^l M_x^P \frac{\partial^2 N_i}{\partial x^2}\,\mathrm{d}x \tag{11}$$

The components of the element stiffness and geometric stiffness matrices are given by

$$K_{ij} = \int_0^l b\bar{D}_{11}\frac{d^2N_i}{dx^2}\frac{d^2N_j}{dx^2}\,\mathrm{d}x \tag{12}$$

$$G_{ij} = \int_0^l bP_x\frac{dN_i}{dx}\frac{dN_j}{dx}\,\mathrm{d}x \tag{13}$$

where l is the length and b is the width of the laminated beam and N_i denotes the interpolation functions given by

$$N_1 = 1 - 3\left(\frac{x}{l}\right)^2 + 2\left(\frac{x}{l}\right)^3; \qquad N_2 = -x + 2x\left(\frac{x}{l}\right) - x\left(\frac{x}{l}\right)^2$$
$$N_3 = 3\left(\frac{x}{l}\right)^2 - 2\left(\frac{x}{l}\right)^3; \qquad N_4 = x\left(\frac{x}{l}\right) - x\left(\frac{x}{l}\right)^2 \tag{14}$$

where $P_x = P_x^M + P_x^p$, represents the axial force where P_x^M is the mechanical axial force and P_x^p is the axial force due to the applied voltage on the piezoelectric actuators given by Eq. (8a).

The components of the element mass matrix of the beam is given by

$$M_{ij} = \int_0^l \left(I_1 N_i N_j + I_2\frac{dN_i}{dx}\frac{dN_i}{dx}\right)\mathrm{d}x \tag{15}$$

where I_1 and I_2 are the mass moment of inertias that can be obtained by

$$I_1, I_2 = \int_{-\frac{h}{2}}^{\frac{h}{2}} b\rho(1, z^2)\,\mathrm{d}z \tag{16}$$

It is noted that superscript "e" has been dropped from Eqs. (11–13) and (15) for the sake of clarity.

B. First-Order Shear Deformation Theory

The first-order shear deformation theory (FSDT) improves the classical laminated theory (CLT) by introducing the effects of transverse shear deformation. The displacements field based on FSDT is given as follows:

$$u(x, z, t) = u_0(x, t) + z\phi_x(x, t), \qquad w(x, z, t) = w_0(x, t) \tag{17}$$

where (u_0, w_0) are the displacements of a point on the midplane surface $z = 0$, ϕ_x is the rotations of transverse normal about the y axis. Using the Hamilton principle, Eq. (9), and the finite element method, the governing equations of motion for the laminated composite beam based on the first-order shear deformation theory can be derived in matrix form as [15]:

$$\begin{bmatrix}[K^{11}] & [K^{12}]\\ [K^{12}]^T & [K^{22}]\end{bmatrix}^e\begin{Bmatrix}\{w\}\\ \{\phi\}\end{Bmatrix}^e + \begin{bmatrix}[G] & [0]\\ [0] & [0]\end{bmatrix}^e\begin{Bmatrix}\{w\}\\ \{\phi\}\end{Bmatrix}^e$$
$$+\begin{bmatrix}[M^{11}] & [0]\\ [0] & [M^{22}]\end{bmatrix}^e\begin{Bmatrix}\{\ddot{w}\}\\ \{\ddot{\phi}\}\end{Bmatrix}^e = \begin{Bmatrix}\{F^1\}\\ \{F^2\}\end{Bmatrix}^e + \begin{Bmatrix}\{0\}\\ \{F_S^P\}\end{Bmatrix}^e - \begin{Bmatrix}\{0\}\\ \{F_B^P\}\end{Bmatrix}^e \tag{18}$$

where the coefficients of the above element matrices are given by (superscript e has been dropped for the sake of clarity):

$$G_{ij} = \int_0^l bP_x\frac{\mathrm{d}S_i}{\mathrm{d}x}\frac{\mathrm{d}S_j}{\mathrm{d}x}\mathrm{d}x \tag{19}$$

$$K_{ij}^{11} = \int_0^l b\mu F_{55}\frac{\mathrm{d}S_i}{\mathrm{d}x}\frac{\mathrm{d}S_j}{\mathrm{d}x}\mathrm{d}x \tag{20}$$

$$K_{ij}^{12} = \int_0^l b\mu F_{55}\frac{\mathrm{d}S_i}{\mathrm{d}x}\varphi_j\,\mathrm{d}x \tag{21}$$

$$K_{ij}^{22} = \int_0^l\left[b\bar{D}_{11}\frac{\mathrm{d}\varphi_i}{\mathrm{d}x}\frac{\mathrm{d}\varphi_j}{\mathrm{d}x} + b\mu F_{55}\varphi_i\varphi_j\right]\mathrm{d}x \tag{22}$$

$$M_{ij}^{11} = \int_0^l I_1 S_i S_j\,\mathrm{d}x, \qquad \int_0^l I_2\varphi_i\varphi_j\,\mathrm{d}x \tag{23}$$

where S_i and φ_i are the interpolation functions corresponding to displacements and rotations, respectively, given by

$$S_1 = \varphi_1 = 1 - \frac{x}{l}; \qquad S_2 = \varphi_2 = \frac{x}{l} \tag{24}$$

μ denotes the shear correction factor and F_{55} is determined as

$$F_{55} = \sum_{k=1}^{n+n_p}(h_k - h_{k-1})(\bar{Q}_{55})_k = \sum_{k=1}^{n+n_p}(t_k)(\bar{Q}_{55})_k \tag{25}$$

In the right hand side of Eq. (18), the vector $\{F\}^e$ is the element transverse mechanical load and the vectors $\{F_s^p\}^e$ and $\{F_B^p\}^e$ represent element shear and bending forces due to the piezoelectric actuators, respectively, which their components can be determined by the following expressions [15]:

$$F_{Si}^P = \int_{z_k}^{z_{k+1}} Q_x^P\varphi_i\,\mathrm{d}x, \qquad F_{Bi}^P = \int_0^l M_x^P\frac{\partial\varphi_i}{\partial x}\,\mathrm{d}x \tag{26}$$

where Q_x^P represents the transverse shear force due to piezoelectric actuators and can be calculated from the following equation:

$$Q_x^P = \sum_{k=1}^{n+n_p}\int_{z_{k-1}}^{z_{kk}} b\bar{Q}_{55}d_{15}^{(k)}E_x^{(k)}\,\mathrm{d}z \tag{27}$$

where $E_x^{(k)}$ is the electric field applied to the kth layer of piezoelectric actuators in the x direction and $d_{15}^{(k)}$ is the piezoelectric constant. In this work it is assumed that the electric field is only applied through the thickness, thus $E_x = 0$ and subsequently $Q_x^p = 0$ and $F_{S\,i}^P = 0$.

III. Design Optimization

To determine the optimal design of laminated beam with integrated piezoelectric actuators, one of the most powerful methods of the gradient based optimization techniques, namely the SQP method has been implemented. For more details of the procedure one may consult the books written by Arora [17] and Fletcher [18]. For the sake of self-contentedly of the article, here the most essential issues of the SQP technique have been reviewed. The main idea is to generate a quadratic programming (QP) problem based on a quadratic approximation of the Lagrangian function described as [17]:

$$L(\{q\}, \lambda) = f(\{q\}) + \sum_{i=1}^{m}\lambda_i.g_i(\{q\}) \tag{28}$$

where $\{q\}$, g_i, and λ_i are design variable vector, constraints, and Lagrange multipliers, respectively. It should be noted that the bound constraints have been expressed as inequality constraints in derivation of the Lagrangian in Eq. (28). The SQP implementation consists of three main steps: 1) a QP subproblem solution; 2) a line search and objective function calculation, and 3) updating of the

Hessian matrix of the Lagrangian function given by Eq. (28). The procedure proceeds by solving a QP subproblem at each major iteration.

The solution of the QP subproblem generates an estimate of the Lagrange multiplier λ and a search direction vector $\{d\}$ in each iteration k, which is used to form a new iteration as

$$\{q\}_{k+1} = \{q\}_k + \alpha_k \{d\}_k \tag{29}$$

The step length parameter α_k, should be determined by using an appropriate line search technique (one-dimensional minimizations) in order to produce a sufficient decrease in the merit function. At the end of the one-dimensional minimization, the Hessian of the Lagrangian, required for the solution of the next positive definitive quadratic programming problem, is updated using the Broyden–Fletcher–Goldfarb–Shanno (BFGS) updated formula [18].

For the solution of QP subproblem, the algorithm requires computing the gradient of both constraints and objective function at each iteration. Gradients are typically evaluated using finite difference method. It has been shown that the results obtained based on the analytical gradients lead to faster convergence and more accuracy. According to the best knowledge of the authors, analytical gradients of stress, displacement and frequency constraints in laminated composite beams with piezoelectric patches have not been reported in the literature.

It should be noted that the nonlinear mathematical programming optimization techniques such as SQP may find the local minima instead of the global one. In other words, they may get trapped into the local optima, without having a mechanism to climb out of it. Thus, these methods may fail to discover the global optimum. In this study, to alleviate this problem, optimization algorithm has been executed for multitude of random initial points in an attempt to catch the global optimum point. It is noted that in this study the design vector $\{q\} = \{t_1, t_2, \ldots, t_{n+n_p}\}$ consists of thicknesses of composite layers and piezoelectric actuators.

IV. Gradient Evaluations of Constraints

From the previous section, it was realized that the gradient evaluation of both objective function and constraints is of essential importance to improve the accuracy of the optimization results. Most of the design optimization algorithms for laminated composites have been developed based on the numerical approximation of the gradient of constraints. The analytical gradient evaluation of constraints may significantly improve the accuracy and convergence of the results. This improvement may also reduce the computational time significantly. One of the main objectives of this study is to develop analytical formulation for the gradient of different constraints using finite element method based on the CLT and FSDT theories and to realize their effects in different practical design optimization problems. In the following sections, the analytical expressions for the gradient of stress, displacement and frequency constraints of smart laminated beams have been developed based on the finite element formulation.

A. Gradient of Stress and Displacement Constraints

Using the displacement method of analysis, the finite element technique requires the solution of the following matrix equation in static problems

$$[K]_{\text{eq}}\{U\} = \{F\} + \{F^P\} \tag{30}$$

where $\{U\}$ is the nodal displacement vector and $[K]_{\text{eq}}$ is the equivalent stiffness matrix which is given by

$$[K]_{\text{eq}} = [K] + [G] \tag{31}$$

where $\{F\}$ and $\{F^P\}$ represent the mechanical and piezoelectric load vectors, respectively. It is noted that in design optimization problems, the nodal displacement vector, $\{U\}$ is an implicit function of design variable vector, $\{q\}$ of the system. Stress is also an implicit function of design variable as it is calculated using the nodal displacements. In general, the stress and displacement related constraints can be written in the following general form:

$$g_i(\{U\}, \{q\}) \le 0, \qquad i = 1, 2, \ldots, m \tag{32}$$

where m is the number of constraints. To use SQP technique or any other modern gradient based optimization method, it is required to evaluate gradient of the constraint functions with respect to design variables, thus by considering Eq. (32), we may write [17]

$$\frac{dg_i}{dq_i} = \frac{\partial g_i}{\partial q_i} + \left(\frac{\partial g_i}{\partial \{U\}}\right)^T \frac{\partial \{U\}}{\partial q_i}$$
$$\text{where } \frac{\partial g_i}{\partial \{U\}} = \left[\frac{\partial g_i}{\partial U_1} \frac{\partial g_i}{\partial U_2} \cdots \frac{\partial g_i}{\partial U_3}\right]^T \tag{33}$$

Calculation of $\partial g_i/\partial q_i$ and $\partial g_i/\partial\{U\}$ are generally straightforward. The term $\partial\{U\}/\partial q_i$ is calculated by differentiating both sides of Eq. (30) with respect to $\{q\}$:

$$[K]_{\text{eq}} \frac{\partial \{U\}}{\partial q_i} = \frac{\partial \{F\}}{\partial q_i} + \frac{\partial \{F^P\}}{\partial q_i} - \frac{\partial [K]_{\text{eq}}}{\partial q_i}\{U\} \tag{34}$$

Assuming external mechanical load vector is independent of design variables, we have $\partial\{F\}/\partial q_i = 0$. Thus Eq. (34) can be written as

$$\frac{\partial \{U\}}{\partial q_i} = [K]_{\text{eq}}^{-1}\left(\frac{\partial \{F^P\}}{\partial q_i} - \frac{\partial [K]_{\text{eq}}}{\partial q_i}\{U\}\right) \tag{35}$$

Considering above, to evaluate the gradient of constraints using Eq. (33), one requires to find gradient of nodal displacement vector. The gradient of nodal displacement vector can be easily obtained using Eq. (35), once the derivative of global stiffness matrix with respect to design variables is known. In the following sections the derivative of the element stiffness matrix using the classical laminate theory and the first-order shear deformation theory is derived. The derivative of the global stiffness matrix can be found by regular finite element assembling procedure. In other word,

$$\frac{\partial [K]_{\text{eq}}}{\partial q_i} = \sum_{e=1}^{NE} \frac{\partial [K]_{\text{eq}}^e}{\partial q_i} \tag{36}$$

In principle, $\partial[K]_{\text{eq}}/\partial q_i$ is of the same dimension as $[K]_{\text{eq}}$. However, considering that usually only a few element are directly influenced by a given design variable, this matrix is quite sparse and multiplication given in Eq. (35) may be done without actually constructing the matrix.

1. *Classical Laminate Theory*

As the design variables are assume to be composite layer thickness and actuators thickness, therefore, the shape functions N_i do not depends on design variables. Therefore, the derivative of the components of the element stiffness matrix can be obtained using Eqs. (12) and (13) as

$$\frac{\partial K_{ij}}{\partial q_i} = \int_0^l b \frac{\partial \bar{D}_{11}}{\partial q_i} \frac{d^2 N_i}{dx^2} \frac{d^2 N_j}{dx^2}\, \mathrm{d}x \tag{37}$$

$$\frac{\partial G_{ij}}{\partial q_i} = \int_0^l b \frac{\partial P_x}{\partial q_i} \frac{dN_i}{dx^2} \frac{dN_j}{dx}\, \mathrm{d}x \tag{38}$$

It should be noted that the electric field is considered a constant value through the thickness. Thus, $\partial P_x/\partial q_i = 0$ and subsequently $\partial G_{ij}/\partial q_i = 0$. For a symmetric laminate, the gradient of $\bar{D}_{11}$ can be determined based on Eq. (7) as follows:

$$\frac{\partial \bar{D}_{11}}{\partial q_i} = \sum_{k=1}^{n+n_p} \bar{Q}_{11}^k \frac{\partial}{\partial q_i}\left(t_k \bar{z}_k^2 + \frac{t_k^3}{12}\right) \tag{39}$$

In fact, the gradient of $\bar{D}_{11}$ is computed by adding analytical derivatives of all plies through the thickness of the laminate, including the piezoelectric layers.

By substituting Eq. (39) and shape function given by Eq. (14) into Eq. (37), gradient of stiffness matrix can be obtained as

$$\frac{\partial[K]}{\partial q_i} = \frac{2b\sum_{k=1}^{n+n_p}\bar{Q}_{11}^k\frac{\partial}{\partial q_i}\left(t_k\bar{z}_k^2+t_k^3/12\right)}{l^3}\begin{bmatrix} 6 & -3l & -6 & -3l \\ & 2l^2 & 3l & l^2 \\ & & 6 & 3l \\ \text{sym} & & & 2l^2 \end{bmatrix} \tag{40}$$

Now, Using Eq. (11), the gradient of actuator force is derived by

$$\frac{\partial\{F^p\}}{\partial q_i} = \int_0^l \frac{\partial M_x^p}{\partial q_i}\frac{\partial^2 N_i}{\partial x^2}\,\mathrm{d}x \tag{41}$$

Finally, the gradient of global stiffness matrix is determined by assembling all the gradients at the element level.

2. First-Order Shear Deformation Theory

Similarly the gradient of the element stiffness matrix based on the first-order shear deformation theory has been determined by differentiation of Eqs. (19–22):

$$\frac{\partial G_{ij}^e}{\partial q_i} = \int_0^l b\frac{\partial P_x}{\partial q_i}\frac{\mathrm{d}S_i}{\mathrm{d}x}\frac{\mathrm{d}S_j}{\mathrm{d}x}\,\mathrm{d}x \tag{42}$$

$$\frac{\partial K_{ij}^{11}}{\partial q_i} = \int_0^l b\mu\frac{\partial F_{55}}{\partial q_i}\frac{\mathrm{d}S_i}{\mathrm{d}x}\frac{\mathrm{d}S_j}{\mathrm{d}x}\,\mathrm{d}x \tag{43}$$

$$\frac{\partial K_{ij}^{12}}{\partial q_i} = \int_0^l b\mu\frac{\partial F_{55}}{\partial q_i}\frac{\mathrm{d}S_i}{\mathrm{d}x}\varphi_j\,\mathrm{d}x \tag{44}$$

$$\frac{\partial K_{ij}^{22}}{\partial q_i} = \int_0^l\left[b\frac{\partial\bar{D}_{11}}{\partial q_i}\frac{\mathrm{d}\varphi_i}{\mathrm{d}x}\frac{\mathrm{d}\varphi_j}{\mathrm{d}x}+b\mu\frac{\partial F_{55}}{\partial q_i}\varphi_i\varphi_j\right]\mathrm{d}x \tag{45}$$

The derivative of F_{55} may be determined from Eq. (25):

$$\frac{\partial F_{55}}{\partial q_i} = \frac{\partial}{\partial q_i}\sum_{k=1}^{n+n_p} t_k(\bar{Q}_{55})_k \tag{46}$$

Considering the thicknesses of the composite lamina t_l and the piezoelectric actuator layer t_p as design variables, Eq. (46) can be evaluated as

$$\frac{\partial F_{55}}{\partial t_l} = \sum_{k=1}^{n}(\bar{Q}_{55})_k, \qquad \frac{\partial F_{55}}{\partial t_p} = \sum_{k=n}^{n+n_p}(\bar{Q}_{55})_k \tag{47}$$

Gradient of stiffness matrix can be obtained by evaluating Eqs. (39) and (47) and substituting into Eqs. (43–45).

$$\frac{\partial[K]}{\partial q_i} = \frac{b\mu}{4l}\begin{bmatrix} 4 & -2l & -4 & -2l \\ & l^2 & 2l & l^2 \\ & & 4 & 2l \\ \text{sym} & & & l^2 \end{bmatrix}\frac{\partial}{\partial q_i}\sum_{k=1}^{n+n_p} t_k(\bar{Q}_{55})_k + \frac{4bt}{l}\begin{bmatrix} 0 & 0 & 0 & 0 \\ & 1 & 0 & -1 \\ & & 0 & 0 \\ \text{sym} & & & 1 \end{bmatrix}\sum_{k=1}^{n+n_p}\bar{Q}_{11}^k\frac{\partial}{\partial q_i}\left(t_k\bar{z}_k^2+t_k^3/12\right) \tag{48}$$

The gradient of the actuator bending force can be derived from Eq. (26) as

$$\frac{\partial\left\{F_B^P\right\}}{\partial q_i} = \int_0^l \frac{\partial M_x^P}{\partial q_i}\frac{\partial\varphi_i}{\partial x}\,\mathrm{d}x \tag{49}$$

B. Gradient of Frequency

The gradient evaluation for frequency constraints can be determined from the following equation [17]:

$$\frac{\mathrm{d}\lambda}{\mathrm{d}\{q\}} = \{\bar{U}\}^T\left(\frac{\mathrm{d}[K]}{\mathrm{d}\{q\}}-\lambda\frac{\mathrm{d}[M]}{\mathrm{d}\{q\}}\right)\{\bar{U}\} \tag{50}$$

where $\lambda=\omega^2$ denote the square root of natural frequency and $\{\bar{U}\}$ is the vector of associated mode shape. The gradients of stiffness for both the classical laminate and first-order shear deformation theories have already been presented in Sec. IV.A. The gradient of mass matrix based on the classical laminate theory can be determined using Eq. (15) as

$$\frac{\partial M_{ij}}{\partial q_i} = \int_0^l\left(\frac{\partial I_1}{\partial q_i}N_iN_j+\frac{\partial I_2}{\partial q_i}\frac{\mathrm{d}N_i}{\mathrm{d}x}\frac{\mathrm{d}N_j}{\mathrm{d}x}\right)\mathrm{d}x \tag{51}$$

Similarly, the gradient of mass matrix based on the first-order shear deformation theory can be determined using Eq. (23) as

$$\frac{\partial M_{ij}^{11}}{\partial q_i} = \int_0^l\frac{\partial I_1}{\partial q_i}S_iS_j\,\mathrm{d}x, \qquad \frac{\partial M_{ij}^{22}}{\partial q_i} = \int_0^l\frac{\partial I_2}{\partial q_i}\varphi_i\varphi_j\,\mathrm{d}x \tag{52}$$

In a similar manner, the gradient of mass matrix based on the classical laminated theory and the first-order shear deformation theory can be obtained by substituting the corresponding shape functions given in Eqs. (14) and (24) in Eqs. (51) and (52), respectively.

If the design variables are other than lamina thickness such as applied voltage, one can easily obtain the gradient of element matrices in a similar manner. For example, if the design variable is only voltage of actuator, V, then the gradient of stiffness and mass matrices are zero with respect to voltage. Therefore, the gradient of nodal displacements can be reduced to

$$\frac{\partial\{U\}}{\partial V} = [K]_{\text{eq}}^{-1}\left(\frac{\partial\{F^P\}}{\partial V}\right) \tag{53}$$

where $\{F^P\}$ is a linear function of applied voltage and its gradient can easily be obtained.

V. Validation of the Finite Element Model

To validate the finite element model, a benchmark static problem has been solved and the results have been compared with the published results. In this example, a cross-ply symmetric laminated composite beam [0/90/90/0], made of graphite/epoxy plies (AS/3501) with two layers of piezoceramic actuators (G1195), bonded on top and bottom surfaces of the beam, is considered. The material properties of piezoelectric actuators (G1195) are $E_1=E_2=$ 63.0 GPa, $G_{12}=24.8$ GPa, $v_{12}=0.28$, $d_{31}=d_{32}(\text{m/V})=-166.0\times10^{-12}$ and that of graphite/epoxy (AS/3501) are

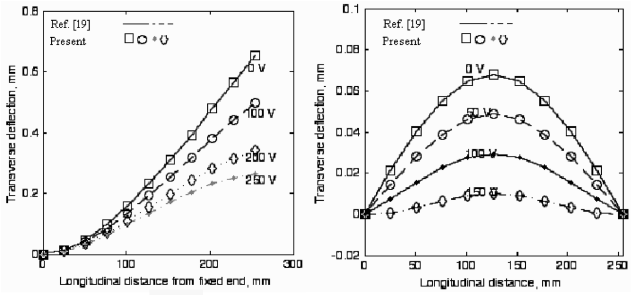

a) b)

Fig. 2 Effect of actuator voltage on transverse deflection of a) cantilever and b) simply-supported beam.

$E_1 = 144.8$ GPa, $E_2 = 9.65$ GPa, $\nu_{12} = 0.3$, $G_{12} = 7.1$ GPa, $G_{23} = 5.92$ GPa. The length and width of the beam are 0.254 and 0.0254 m, respectively. The thicknesses for each layer of the actuator and the composite are 0.2 and 1.27 mm, respectively. Deflection of the beam with a uniformly distributed load of $q_0 = 2 \times 10^3$ N/m^2 and clamped-free and simply-supported boundary conditions, for different applied voltages has been determined using both classical laminate theory and first-order shear deformation theory. Since the problem at hand is relatively thin, the difference between the two theories is negligible. However, for more accuracy, all numerical examples illustrated in the proceeding sections have been solved using the first-order shear deformation theory. The present results have been validated by comparison with published results conducted by Donthireddy and Chandrashekhara [19] as shown in Fig. 2. It must be noted that for the clamped-free beam, the top layer is polarized in the direction of the applied voltages and the bottom layer is polarized in the direction opposite to that of the applied voltage and for the simply-supported beam, the polarity is reversed.

As it can be observed, the results totally match with those in the literature [19]. Thus the finite element models are validated and the analysis model can be used with confidence in design optimization algorithm.

VI. Illustrative Design Optimization Examples

Laminated smart beams can be designed for various purposes. In this section, the optimal design of the laminated composite beams with bounded piezoelectric patches as actuators has been obtained for different applications. A variety of objective functions with different design variables and constraint conditions have been investigated. The first category of the problems is to control the desired geometry of the beams. In these problems, the mean-square error between the actual and the desired shape of the beams has been minimized where the applied voltage on the actuators are considered as design variables. The constraints are upper and lower limits on the design variables. The next category of design optimization problems is aimed to minimize the mass of the piezolaminated beam subjected to different types of loadings under displacement and frequency constraints. The design variables in this set of problems are the thickness of both piezoelectric layers and composite laminas. Material properties for all the examples can be found in Table 1.

Table 1 Material properties

	PC5K Lead zirconate titanate	S-Glass/Epoxy
E_1 (N/m^2)	60.24×10^9	55.0×10^9
E_2 (N/m^2)	60.24×10^9	16×10^9
G_{12} (N/m^2)	23.0×10^9	7.6×10^9
ν_{12}	0.31	0.28
G_{13} (N/m^2)	——	7.6×10^9
G_{23} (N/m^2)	——	7.6×10^9
d_{31} m/V	-306.0×10^{-12}	——
d_{32} m/V	-306.0×10^{-12}	——
ρ (Kg/m^3)	7600	2000.0

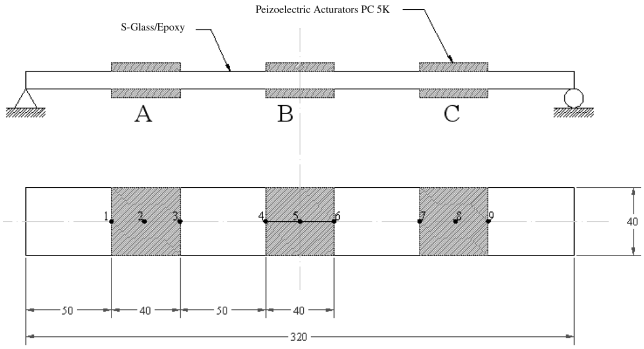

Fig. 3 A simply-supported beam with three pairs of piezoelectric actuator patches.

A. Shape Control Optimizations

1. Optimal Voltage in Simply-Supported Beam

This example is used to investigate the application of the static shape control optimization for a simply-supported beam. For this purpose, a simply-supported beam, with three pairs of surface bonded piezoelectric actuators, as shown in Fig. 3, is subjected to a uniform load of 1000 N/m^2 and transverse deflections in certain control points are measured. It should be noted that shape control has numerous applications in space antennas and telescopic mirrors. It is often required to have desired configuration for the supporting systems of these devices which may be achieved using distributed piezoelectric actuators.

The objective of this problem is to find the appropriate electric voltages that should be applied to the three pairs of piezoelectric actuators in order to minimize the mean-squared error between the actual shape and the desired shape of the beam while the upper and lower limits of ± 200 V are considered for the applied voltages. This problem can be expressed as

$$\min f\left(\sum_{i=1}^{n}[d_i - w_i]^2\right), \qquad \text{subject to: } V_i^l \le V_i \le V_i^u$$
$$i = 1, 2, \ldots, n \qquad g_j(V, w) \le 0, \qquad j = 1, 2, \ldots, m \tag{54}$$

where d_i and w_i represent, respectively, desired and actual transverse displacements, V_i^l and V_i^u are the lower and upper limits for applied voltage, respectively, g_j are the inequality constraints, and n and m represent number of designed variables and number of inequality constraints.

The deflections are measured in 9 control points along the beam. Lamination sequence is $[0 \text{ deg} / 45 \text{ deg} / -45 \text{ deg}]_S$ and the beam is made of S-glass/epoxy layers with surface mounted PC5K (lead zirconate tiatnate) actuators. The initial thicknesses for both laminate and actuators are considered to be 0.5 mm. The results for initial, optimized, and desired shapes of the beam are presented in Table 2. The appropriate voltages to be applied to each pair of piezoelectric patches to obtain the minimized mean-squared error between the actual and desired shape have been provided in Table 3.

As mentioned before, optimum solution obtained using the gradient based mathematical programming algorithms depends on the initial point and may result in local minima(s). In an attempt to significantly increase the probability to catch the global optimum, a multitude of random initial points are selected and the best solution is obtained, until all optimal solutions converge to one unique solution. Figure 4 shows the iteration history of the objective function of the problem versus number of iteration using different random initial points. In the first attempt, only one random initial point has been taken, consequently, in the other attempts, five, ten, twenty, and more random initial points have been taken, respectively. The optimum point is chosen as the minimum of the minimums. As Fig. 5 indicates, if 20 or more random initial points (for this problem) are being chosen, an optimal solution can be found in every attempt. This technique has been used for all of the optimization problems in the present study, to catch the global optimum.

Table 2 Transverse deflections of the control points of the beam

Control points	1 and 9	2 and 8	3 and 7	4 and 6	5	Mean-squared error %
Desired shape (mm)	0.400	0.580	0.730	0.900	0.920	——
Initial shape (mm) V = 0	0.422	0.564	0.694	0.875	0.883	0.0813
Optimized shape (mm)	0.428	0.573	0.710	0.900	0.919	0.0504
Error (before optimization) %	5.5	2.8	4.9	2.8	4.0	——
Error (after optimization) %	7.0	1.2	2.7	0.7	0.1	——

Table 3 Electric voltages applied to the actuator pairs (V)

Initial design			Final design		
Pair A	Pair B	Pair C	Pair A	Pair B	Pair C
0	0	0	−24.5	75.3	−24.5

It should be noted that the initial shape is selected as a static deflection of the beam under the uniform applied load. The desired shape is basically close to the initial shape as practically it is not possible to change the shape significantly due to small deformation induced by piezoelectric actuators and limited available voltage. One practical application is in space antennas or ground telescopic mirrors. When these devices are attached to the beams under stress, the small change in the shape will significantly change the orientation of the mirror.

2. *Optimal Voltage in Cantilever Beam*

In the present case, shape control procedure has been applied on a cantilever beam with five pairs of piezoelectric actuators as shown in Fig. 6. In this example, six control points, five on midpoint of each actuator and the sixth one on the tip of the beam, are considered to monitor and control the deflections. The upper and lower limits of ±250 V are considered for the applied voltages. The results for the desired and optimized (controlled) shape of the beam are given in Table 4. For clear observation, the results of Table 4 have been presented graphically in Fig. 7. Optimal voltages to achieve the desired shape are given in Table 5.

It can be observed that the desired shape of the beam is achieved within an acceptable tolerance, using the five pairs of piezoelectric actuators. Thus the finite element model developed in Sec. II combined with the optimization and sensitivity analysis presented in Secs. III and IV can predict efficiently and accurately the required voltages to be applied on piezoceramic actuators (within the reach of the actuators power) in order to achieve a prescribed desired shape for the adaptive laminated composite beam.

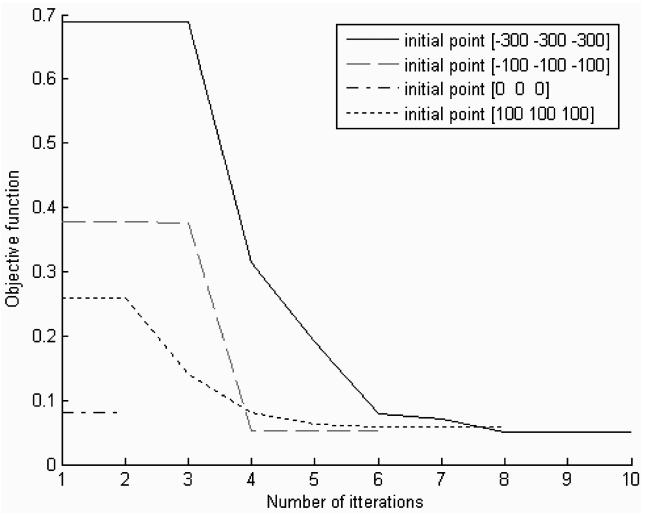

Fig. 4 Iteration histories using various initial points.

B. Mass Minimization of a Piezolaminated Beam

In the following examples, the overall mass of a piezolaminated beam is subjected to minimization by changing the thicknesses of both composite layers (S-glass/epoxy) and piezoelectric actuators (PC5K), while different constraints are applied for each optimization.

It should be noted that piezoelectric actuators can be used to create bending moment and axial force. The bending moment is created by polarizing the top layer in the direction of the applied voltage and the bottom layer in the direction opposite to that of the applied voltage while stretching or axial force is created by polarizing both actuators in the direction of the applied voltage.

1. *Minimizing the Mass of the Smart Cantilever Beam under Static Deflection Constraint*

In the first optimization of this set, the mass of a cantilever smart composite beam subjected to a tip point load of 100 N as shown in Fig. 8 is to be minimized, while the tip deflection of the beam, measured at the point 1, should remain smaller than 0.5 mm. Half of the beam's length is covered with piezoelectric actuators. The beam is made from 6 layers. The thicknesses for composite layers and

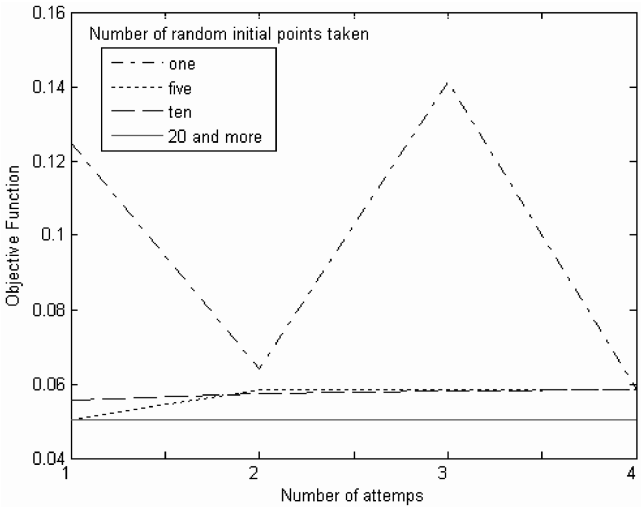

Fig. 5 The effect of number of random initial points taken on the chance of finding global minimum.

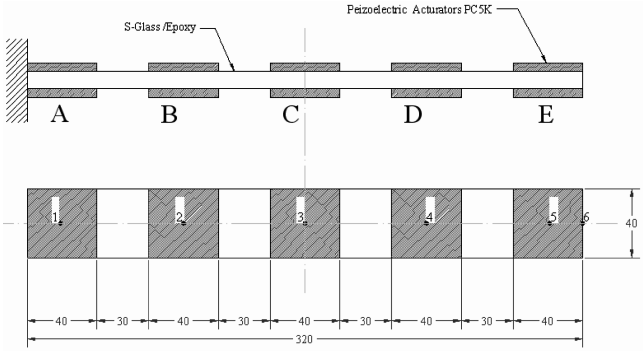

Fig. 6 A cantilever beam with five pairs of piezoelectric actuator patches.

Table 4 Transverse deflections of the control points of the beam (desired shape I)

Control points	1	2	3	4	5	6	Mean-squared error
Desired shape I (mm)	−0.006	−0.100	0.000	0.100	0.200	0.250	——
Initial shape (mm) V = 0	0.000	0.000	0.000	0.000	0.000	0.000	0.350
Optimized shape (mm)	−0.008	0.100	0.000	0.100	0.200	0.250	0.002

Table 5 Electric voltages applied to the actuator pairs (V)

Initial design					Final design				
Pair A	Pair B	Pair C	Pair D	Pair E	Pair A	Pair B	Pair C	Pair D	Pair E
0.0	0.0	0.0	0.0	0.0	101.4	−204.2	17.3	−0.2	−123.7

Table 6 Initial and optimum results for smart cantilever beam under displacement constraint

Initial values			Optimized values		
Thicknesses		Mass (g)	Thicknesses		Mass (g)
Composite layers (mm)	Actuators (mm)		Composite layers (mm)	Actuators (mm)	
4.6	4.5	908.8	5.472	0.100	570.115

piezoelectric actuator patches are considered as design variables and are initially set at 4.6 and 4.5 mm, respectively. The total initial mass of the beam is 0.909 kg. The optimization results are provided in Table 6. The optimum mass has found to be 0.570 kg. It must be noted that the voltage of 240 V is applied to the actuators in order to maintain the deflection of the beam within the allowable limits. The lower limit of 0.1 mm is considered for both laminate and actuator's thicknesses. The lay-up sequence is $[0/90]_S$.

Results show that at the optimum configuration the tip deflection is −0.5 mm, therefore the displacement constraint is active.

To investigate the effect of evaluation of gradient of the constraint using the finite difference and analytical approach on the optimum results and iteration number, the problem has been solved using both the finite difference and analytical gradients developed in Sec. IV and iteration histories are shown in Fig. 9. It can be realized that integrating the developed analytical gradient formulation into optimization algorithm can significantly reduce the number of iteration and thus the computational time.

As it can be realized from Fig. 9, the optimum results obtained from analytical gradient and finite difference approaches are more or less the same. Using small step size in finite difference will produce accurate result; however, from other side it will increase the computational cost. In this problem, the step size in finite difference approach has been selected in a way that the optimum result obtained by the finite difference to be the same as that of the analytical approach in order to compare the number of optimization iterations. As it can be seen, in order to obtain the same accuracy, finite difference requires much higher number of iterations with respect to that of analytical approach.

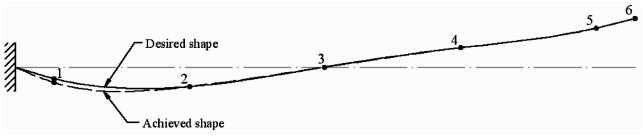

Fig. 7 Desired and achieved shape of a cantilever beam.

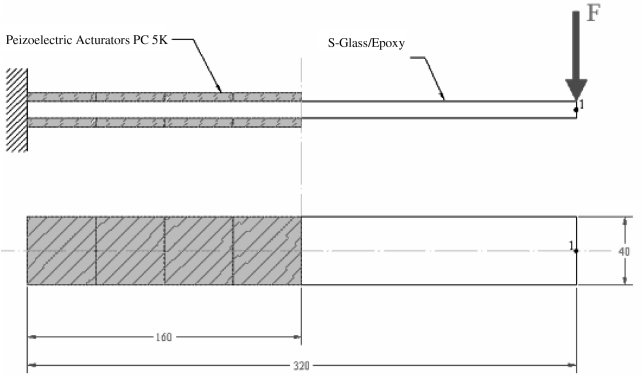

Fig. 8 A piezolaminated cantilever beam with tip load of 100 N and applied voltage of 240 V.

2. *Minimizing the Mass of Cantilever Smart Composite Beam under Frequency Constraints*

Here a cantilever smart composite beam with three pairs of piezoelectric actuators as shown in Fig. 10 is considered. The laminate is made of 6 layers, each with a thickness of 1 mm and

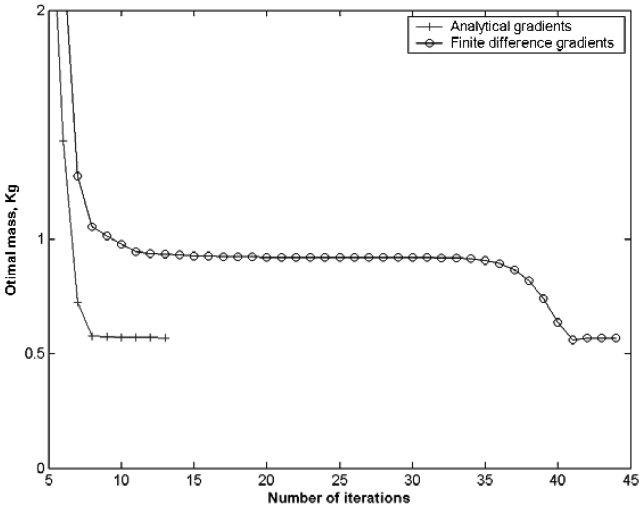

Fig. 9 The iteration histories for the smart cantilever beam, with a tip load of 100 N and applied voltage of 240 V under displacement constraints.

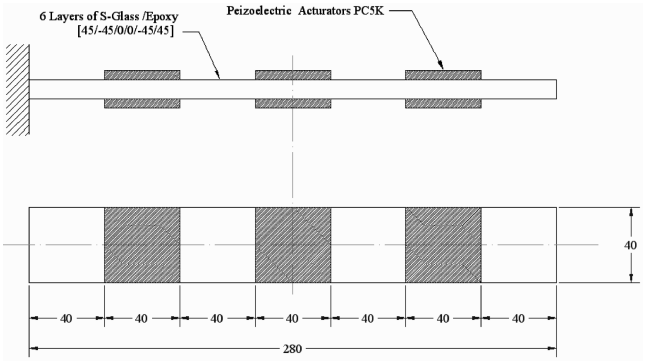

Fig. 10 A piezolaminated cantilever beam, subjected to mass minimization with and without active stiffening.

stacking sequence of $[45/-45/0]_S$. The thickness of each actuator is 0.1 mm. The objective function is to minimize the mass of the structure where the thicknesses of composite layers are considered as design variables and the first three natural frequencies are required to be greater than 40, 215, and 580 Hz, respectively [2]. It should be noted that limits on frequencies are selected arbitrary.

The optimization is being executed once there is no voltage applied on the actuators and the second time when the voltage of 300 V is applied on each pair of actuators in a way that it polarizes both top and bottom actuators in the direction of the applied voltage and therefore, increases natural frequencies of the structures by active stiffening. The results of both optimizations are presented in Table 7. The first three natural frequencies in optimum configuration are found to be 40, 219.5, and 805 Hz for zero V and 43.4, 218.5, and 638 Hz for 300 V. The gradient of constraints has been evaluated using both the finite difference and the developed analytical formulation and the iteration histories are shown in Fig. 11. It can be realized that better optimum result can be achieved by using analytical gradient in optimization algorithm.

3. Minimization of Electric Potential to Suppress Transient Vibration

A cantilever laminated beam with 4 layers [0/90/90/0] each 0.125 mm of thickness. The length and with of the beam are given as 0.25 and 0.0254 m, respectively. The first half from the fixed end of the beam is covered with PZT actuators of 0.1 mm thickness. The beam is subjected to an initial velocity of 1.5 m/s. It is desired to determine the minimum electric potential desired to suppress the transient vibration in a controlled manner. The damping factor of the passive beam in the absence of electric potential applied to the actuators is assumed to 0.1 for all modes. It is required to increase the damping factor to 0.25 by applying electric potential to the actuators. The optimization problem is minimization of error in the response in time interval 0 to T while the absolute amplitude of vibration in this interval should not exceed of 10^{-6} from the response of the system with 0.25 damping coefficient. The problem may cast into the following standard format:

Table 7 Initial and optimum results for smart cantilever beam under frequency constraints

	Thickness (mm)	Overall mass (g)	% Mass reduction
Initial design	1.00	163.32	0
Optimized: without active stiffening (V = 0)			
Finite difference	0.817	135.34	17.13
Analytical gradient	0.800	132.32	18.96
Optimized: with active stiffening (V = 300 V)			
Finite difference	0.734	122.41	25.04
Analytical gradient	0.716	119.71	26.71

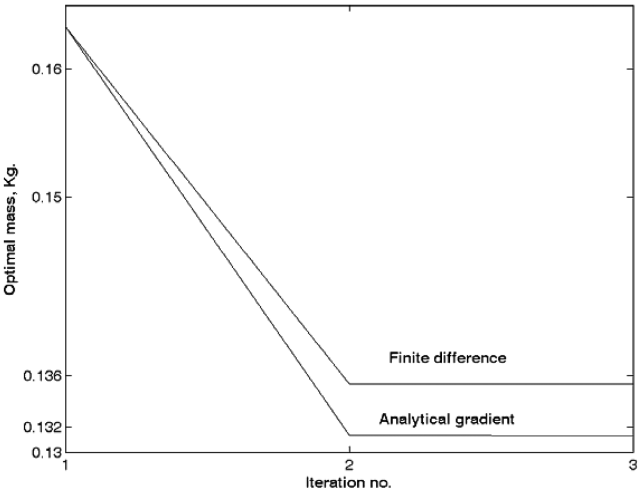

Fig. 11 The iteration histories for the smart cantilever beam under frequency constraints.

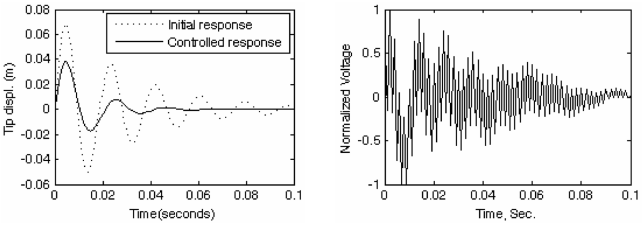

a) **b)**

Fig. 12 a) Vibration suppression using optimal electric potential; b) optimal voltages applied at actuators.

$$\min f = \int_0^T q^2(t)\,\mathrm{d}t \qquad \text{subject to } |q(t)| \le q_a(t)$$
$$q(T) = 0, \qquad |V(t)| \le V_a \tag{55}$$

where q_a is the allowable displacement of the system which is defined by the desired response of the system. T is the allowable time to suppress the motion given as 0.1 sec, V_a is the maximum applied voltage on the actuators. An analytical gradient approach using layerwise theory combined with SQP has been used to find the optimum results. Figure 12a shows the initial response of the laminated beam and the response of the system after the optimum voltages given in Fig. 12b are applied to the system. It is observed that by performing the optimization technique, the vibration is damped out in well controlled manner. It should be noted that in Fig. 12b, the applied voltage in time interval 0 to 0.1 sec is normalized with respect to maximum voltage.

VII. Concluding Remarks

In this study, the finite element model has been derived to investigate the static and dynamic interaction between piezoelectric actuators and host laminated composite structure using classical lamination and first-order shear deformation theories. Piezoelectric actuators have been used to create bending moment for shape control purposes as well as active stiffening to change the natural frequencies.

A formal design optimization algorithm has been developed in which the finite element method has been combined with the sequential programming technique. To improve the convergence and accuracy of the optimization procedure, the analytical gradients of constraints for both static problems as well as frequency constraints have been developed. Two sets of constrained optimizations have been performed: 1) shape control problems in which the mean-square error between the actual and desired shape has been minimized while the applied voltages to actuators have been considered as the design

variables, and 2) mass minimization problems in which the mass of the smart composite beam has been subjected to minimization by changing the thickness of composite layers and/or piezoelectric actuators. In both cases, different constraints have been introduced to the optimization problems. It has been observed that using an analytical gradient may significantly increase the convergence and accuracy of the results.

Acknowledgement

Support by the Natural Science and Engineering Research Council of Canada is gratefully acknowledged.

References

[1] Reddy, J. N., "On Laminated Composite Plates with Integrated Sensors and Actuators," *Engineering Structures*, Vol. 21, No. 7, 1999, pp. 568–593.

[2] Soares, C. M. M., Soares, C. A. M., and Correia, V. M. F., "Optimal Design of Piezolaminated Structures," *Composite Structures*, Vol. 47, No. 1–4, 1999, pp. 625–34.

[3] Correia, V. M. F., Gomes, M. A. A., Suleman, A., Soares, C. M. M., and Soares, C. A. M., "Modeling and Design of Adaptive Composite Structures," *Computer Methods in Applied Mechanics and Engineering*, Vol. 185, Nos. 2–4, 2000, pp. 325–46.

[4] Birman, V., and Simonyan, A., "Optimum Distribution of Smart Stiffeners in Sandwich Plates Subjected to Bending or Forced Vibrations," *Composites, Part B*, Vol. 27, No. 6, 1996, pp. 657–65.

[5] Bruant, I., Coffignal, G., and Lene, F., "A Methodology for Determination of Piezoelectric Actuator and Sensor Location on Beam Structures," *Journal of Sound and Vibration*, Vol. 243, No. 5, 2001, pp. 861–882.

[6] Soares, C. A. M., Soares, C. M. M., and Correia, V. M. F., "Modeling and Design of Laminated Composite Structures with Integrated Sensors and Actuators," *Computational Mechanics for the Twenty-First Century*, Edinburgh, U.K., 2000, pp. 165–185.

[7] Yan, Y. J., and Yam, L. H., "Mechanical Interaction Issues in Piezoelectric Composite Structures," *Composite Structures*, Vol. 59, No. 1, 2003, pp. 61–65.

[8] Barboni, R., Mannini, A., Fantini, E., and Gaudenzi, P., "Optimal Placement of PZT Actuators for the Control of Beam Dynamics," *Smart Materials and Structures*, Vol. 9, No. 1, 2000, pp. 110–120.

[9] Batra, R. C., and Geng, T. S., "Enhancement of the Dynamic Buckling Load for a Plate by using Piezoceramic Actuators," *Smart Materials and Structures*, Vol. 10, No. 5, 2001, pp. 925–33.

[10] Correia, V. M. F., Soares, C. M. M., and Soares, C. A. M., "Buckling Optimization of Composite Laminated Adaptive Structures," *Composite Structures*, Vol. 62, Nos. 3,4, 2003, pp. 315–321.

[11] Baz, A., and Poh, S., "Performance of an Active Control System with Piezoelectric Actuators," *Journal of Sound and Vibration*, Vol. 126, No. 2, 1988, pp. 327–343.

[12] Aldraihem, J. O., "Optimal Size and Location of Piezoelectric Actuators/sensors: Practical Considerations," *Journal of Guidance, Control, and Dynamics*, Vol. 23, No. 3, 2000, pp. 509–515.

[13] Suleman, A., and Goncalves, M. A., "Multi-objective Optimization of an Adaptive Composite Beam Using the Physical Programming Approach," *Journal of Intelligent Material Systems and Structures*, Vol. 10, Jan. 1999, pp. 56–70.

[14] Frecker, M. I., "Recent Advances in Optimization of Smart Structures and Actuators," *Journal of Intelligent Material Systems and Structures*, Vol. 14, April 2003, pp. 207–216.

[15] Reddy, J. N., *Mechanics of Laminated Composite Plates—Theory and Analysis*, CRC Press, Boca Raton, Florida, 1997.

[16] Bertholet, J. M., *Composite Materials—Mechanical Behavior and Structural Analysis*, Springer–Verlag, New York, 1999.

[17] Arora, J. S., *Introduction to Optimum Design*, Elsevier Academic Press, San Diego, California, 2004.

[18] Fletcher, R., *Practical Methods of Optimization*, 2nd ed., John Wiley, Chichester, U.K., 1987.

[19] Donthireddy, P., and Chandrashekhara, K., "Modeling and Shape Control of Composite Beams with Embedded Piezoelectric Actuators," *Composite Structures*, Vol. 35, No. 3, 1996, pp. 237–244.

A. Roy
Associate Editor